JOURNAL
OF THE AMERICAN CHEMICAL SOCIETY

Registered in U. S. Patent Office.

VOLUME 89, NUMBER 18 AUGUST 30, 1967

Physical and Inorganic Chemistry

The Study of Ion–Molecule Reactions in Chloroethylene by Ion Cyclotron Resonance Spectroscopy

J. L. Beauchamp,[1] L. R. Anders, and J. D. Baldeschwieler

Contribution from the Department of Chemistry, Stanford University, Stanford, California. *Received February 6, 1967*

Abstract: Bimolecular ion–molecule reactions in chloroethylene have been studied using ion cyclotron single- and multiple-resonance techniques. Consecutive reactions are followed to a high order at low pressure by appropriate ion-trapping conditions. The most general reaction observed is of the type $A^+ + C_2H_3Cl \rightarrow AC_2H_2^+ + HCl$. The reaction of $C_2H_3Cl^+$ with C_2H_3Cl yields three products: $C_3H_4Cl^+$, $C_4H_5Cl^+$, and $C_4H_6Cl^+$. In all three cases the chlorine in the product comes with equal probability from the charged or neutral reactant.

I. Introduction

The collision of an ion with a neutral molecule at low pressures can give rise to a generalized bimolecular reaction of the type

$$A^+ + B \longrightarrow C^+ + D \qquad (1)$$

Reactions of this type frequently involve the formation of a chemically interesting intermediate species which rapidly fragments in the absence of a stabilizing collision. The nature of the intermediate species and the fragments into which it decomposes have become a popular subject for theoretical and experimental analysis.[2] For example, the phase space theory of chemical kinetics developed by Light[3] and his-co-workers appears to give an adequate description of three-body ion–molecule reactions, and will undoubtedly be extended with approximations to predict the decomposition of larger intermediate complexes. The experimental techniques available for the study of ion-molecule reactions have been reviewed by various authors,[2] and recent interest has been sufficient to warrant the publication of a monograph on the subject.[4] Tandem mass spectrometers, for example, provide a wealth of data on various aspects of primary ion–molecule reactions.[5,6] However the available techniques have not been particularly suitable for the study of complex, high-order ion–molecule reaction sequences. Ion cyclotron resonance provides a straightforward method which uniquely fulfills this need.

Ion cyclotron resonance spectroscopy (icr) is based on the classical motion of charged particles in magnetic and electric fields. The motion of a free charged particle in a uniform magnetic field is constrained to a circular orbit of angular frequency ω_c in a plane normal to **H**, and is unrestricted parallel to **H**. The cyclotron frequency, ω_c, is independent of velocity and is given in gaussian cgs units by

$$\omega_c = eH/mc \qquad (2)$$

where e is the charge of the particle, H the magnetic field strength, m the particle mass, and c the speed of light. The radius of the circular motion is given by

$$r = v_\perp/\omega_c \qquad (3)$$

where $v_\perp$ is the component of ion velocity in the plane

---

(1) National Science Foundation Predoctoral Fellow, on Traveling Guidance from Harvard University.

(2) (a) F. W. Lampe, J. L. Franklin, and F. H. Field, *Progr. Reaction Kinetics*, **1**, 68 (1961); (b) C. F. Giese, *Advan. Chem. Phys.*, **10**, 247 (1966).

(3) J. Lin and J. Light, *J. Chem. Phys.*, **45**, 2545 (1966).

(4) "Ion-Molecule Reactions in the Gas Phase," Advances in Chemistry Series, No. 58, American Chemical Society, Washington, D. C., 1966.

(5) E. Lindholm, ref 4, Chapter 1.

(6) L. W. Sieck, F. P. Abramson, and J. H. Futrell, *J. Chem. Phys.*, **45**, 2859 (1966).

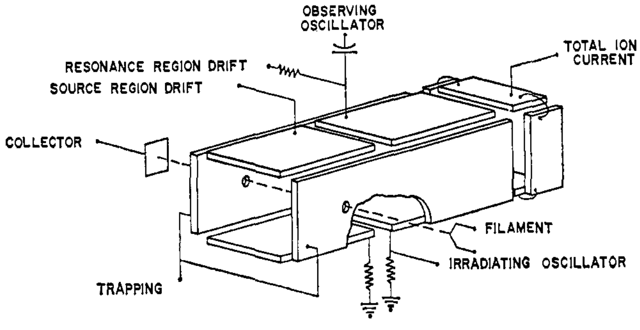

Figure 1. Cutaway view of cyclotron resonance cell. The electron beam is collinear with the magnetic field.

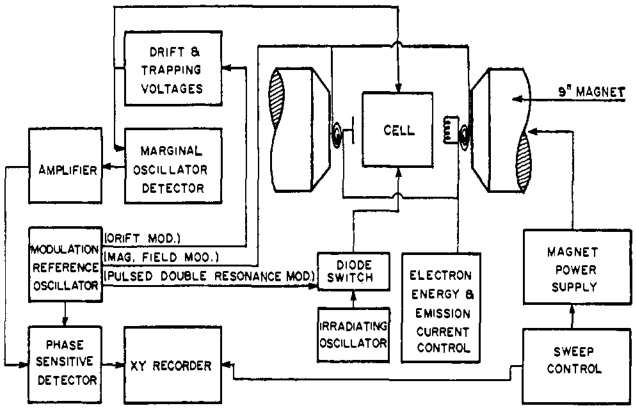

Figure 2. Block diagram of cyclotron resonance apparatus.

perpendicular to the field direction. Typical values for these parameters are, in the case of argon ions at thermal energies in an 8-kgauss field, $\omega_c = 307$ kc/sec and $r = 0.02$ cm. When an alternating electric field, $\mathbf{E}_1(t)$ at frequency ω_1, is applied normal to $\mathbf{H}$ with $\omega_1 = \omega_c$, an absorption of energy by the ions occurs which can be readily observed using a marginal oscillator–detector. With a fixed observing frequency, a spectrum linear in mass can be obtained by sweeping the magnetic field.

In an ionized gas at a pressure where a reaction of the type 1 occurs, both C^+ and A^+ can be detected by the observing oscillator–detector. A second alternating electric field, $\mathbf{E}_2(t)$ at frequency ω_2, applied at the cyclotron frequency of A^+ can cause a significant change in the rate of reaction 1 by heating the reactant ion. This results in an easily detectable change in the measured absorption of energy by the product C^+ from $\mathbf{E}_1(t)$. This double-resonance technique has been successfully applied to the study of charge exchange among isotopes of the rare gases[7] and to the reaction[8]

$$CD_4^+ + N_2 \longrightarrow N_2D^+ + CD_3 \qquad (4)$$

for which an increase in the N_2D^+ absorption was effected by irradiating CD_4^+. Ion cyclotron multiple resonance thus provides a simple means of identifying reactant ions in a reaction mixture, even in the presence of competing processes.

This paper illustrates the application of cyclotron resonance techniques to the study of ion–molecule reactions in chloroethylene. The apparatus and experimental conditions are described in detail in section II. The rather complex scheme of sequential ion–molecule reactions occuring in chloroethylene is analyzed in section III, with the significance of some of the reactions of interest being considered in detail in section IV.

II. Experimental Section

The basic ion cyclotron resonance spectrometer utilized in these experiments was constructed by Varian Associates.[9] As this is the first report of an extensive study of ion chemistry employing cyclotron resonance techniques, a complete description of the apparatus is given.

A cutaway view of the cyclotron resonance cell is shown in Figure 1. The cell is divided equally into a source and resonance region with over-all dimensions of 2.54 × 2.54 × 12.7 cm. Electrons from a rhenium filament are accelerated in the direction of the magnetic field by a negative bias on the filament and enter the source region of the resonance cell through the side plate. The electron beam traverses the source region and is measured on a collector biased at +20 v with respect to the resonance cell. The emission current is operated between 0.1 and 10 μa and is regulated to maintain a constant value as the magnetic field is swept. Trapping voltages applied to the side plates constrain the ion motion in the direction of the magnetic field. Ions are drifted from the source into the resonance regions by the application of static voltages to the top plates of the cell. The drift velocity in the crossed field geometry is in a direction perpendicular to both the magnetic and static electric fields with a magnitude given by[10]

$$v_d = \frac{cE_s}{H} \qquad (5)$$

where E_s is the static electric field strength. Since v_d is independent of charge, both negative and positive ions move in the same direction. With typical values for H and E_s of 5 kgauss and 0.25 v/cm, respectively, $v_d = 5.0 \times 10^3$ cm/sec. Separation of positive and negative ions is effected by selecting the appropriate sign for the trapping voltage. Separate drift voltages are applied to the resonance and source regions to isolate the observing oscillator from the source region and the effects of the electron beam. The top and bottom plates of the resonance region form part of the capacitance in the tank circuit of a marginal oscillator. The marginal oscillator is chosen for its high sensitivity in detecting small impedance changes[11] in the tank circuit. The irradiating oscillator is usually operated at a level above that of the observing oscillator. The simple method of coupling the irradiating voltage to the resonance cell shown in Figure 1 provides adequate decoupling of the irradiating and detecting circuits.

A block diagram of the apparatus is given in Figure 2. The resonance cell is placed between the pole caps of a Varian Associates 9-in. electromagnet with a 1.75-in. gap. The output of the marginal oscillator–detector is amplified and fed to a phase-sensitive detector. The phase-sensitive detector is referenced to a modulation oscillator which provides the three modulation options shown in Figure 2. The first scheme involves modulation of the magnetic field with Helmholtz coils located on the pole caps. The field-modulation method operates in the same fashion as it does when applied to nuclear magnetic resonance and electron paramagnetic resonance.[12] The level of the modulation is adjusted below the point where distortion of the line shape occurs. The spectra thus obtained are insensitive to the ion distribution in the resonance probe. Figures 3 and 4 display typical field-modulation spectra with the characteristic derivative line shapes.

The second of these schemes involves modulation of the drift voltages. This causes a variation in the ion transit time and thereby provides a modulation of the ion number density in the cell. The resulting absorption spectra are as shown in Figure 5. The phase of the signal arising from drift modulation is very sensitive to the ion distribution along the length of the cell. At low pressure the distribution is uniform. This uniformity is disrupted by reactions

---

(7) L. R. Anders, J. L. Beauchamp and J. D. Baldeschwieler, *J. Chem. Phys.*, in press.

(8) L. R. Anders, J. L. Beauchamp, R. C. Dunbar, and J. D. Baldeschwieler, *ibid.*, **45**, 1062 (1966).

(9) Syroton mass spectrometer, Varian Associates, Palo Alto, Calif.

(10) J. D. Jackson, "Classical Electrodynamics," John Wiley and Sons, Inc., New York, N. Y., 1962, p 412.

(11) F. N. H. Robinson, *J. Sci. Instr.*, **36**, 481 (1959).

(12) "NMR and EPR Spectroscopy," Pergamon Press, New York, N. Y., 1960, Chapter 14.

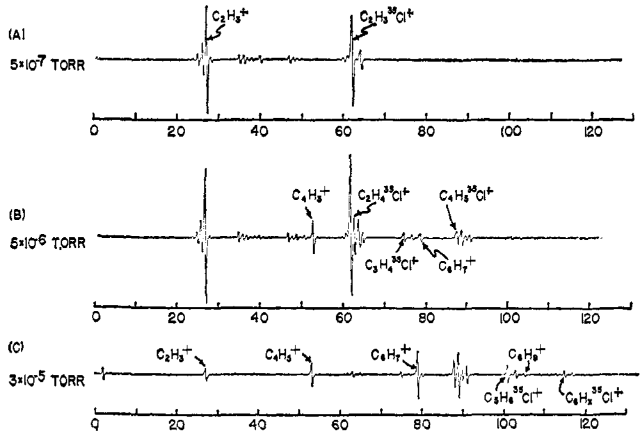

Figure 3. Variation of single-resonance 70-ev electron energy chloroethylene spectra with pressure. For all three spectra ω_1 = 153.0 kc and E_1 = 0.01 v/cm. Field modulation gives the derivative line shape. The most probable ionic species corresponding to a number of peaks are given for reference.

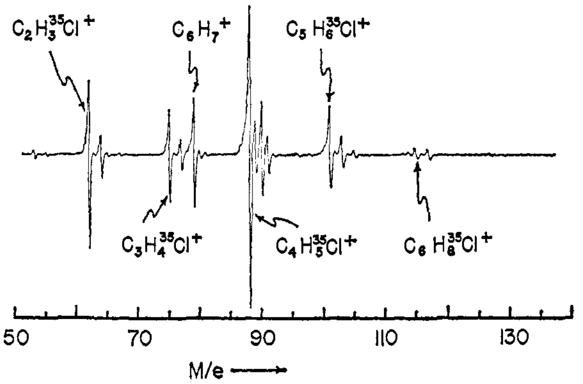

Figure 4. Single-resonance spectrum of chloroethylene with 11-ev electron energy at 3 × 10^{-6} torr pressure. No major peaks were recorded below *m*/*e* 50. The most probable ionic species corresponding to a number of peaks are given for reference.

which occur at higher pressure, the density of reaction products increasing with the distance from the electron beam. Since the reactant density is higher at the entrance to the resonance region, it is not difficult to obtain drift modulation spectra in which the reactant and product peaks are inverted with respect to each other. This situation is not desirable if meaningful intensity measurements are to be made.

The third modulation scheme is an integral part of the highly specific double-resonance technique for identifying ion–molecule reactions. The reference oscillator operates a diode switch which permits square-wave modulation of the irradiating oscillator. The rate of an ion–molecule reaction usually shows *at least* a slight variation with ion energy causing a *change* in number density of product ions when the irradiating oscillator is switched off and on. The modulation information necessary for the marginal oscillator and phase-sensitive detector to produce a signal is thus transmitted only through an ion–molecule reaction. The over-all detection scheme effectively displays the difference between the product ion absorption spectrum with and without reactant irradiation. Figure 6 shows typical pulsed double resonance spectra obtained with frequency sweep of the irradiating oscillator at fixed magnetic field. The dependence of the pulsed double-resonance line shape on the irradiating power has been considered in detail for charge-transfer reactions in mixtures of rare gas isotopes, and bears an interesting analogy to the effects of chemical exchange on nmr and esr line shapes.[7] The modulation frequency employed in all three schemes is ~40 cps.

The resonance probe is contained in a bakeable stainless steel high-vacuum system which can be evacuated to below 10^{-8} torr with an 8-l./sec ion pump. The sample to be studied is admitted through a variable leak valve from a reservoir at 20 torr. All of the spectra discussed were obtained under dynamic conditions with the desired pressure being maintained by varying the leak rate and pumping speed. This prevents accumulation of impurity gases in the system and permits operation of the spectrometer between 10^{-8} and 10^{-2} torr. Pressure measurements were made with an ionization gauge. Since means for accurately calibrating the gauge for chloroethylene in the pressure range employed were not available, the absolute values are probably reliable only to within an order of magnitude.

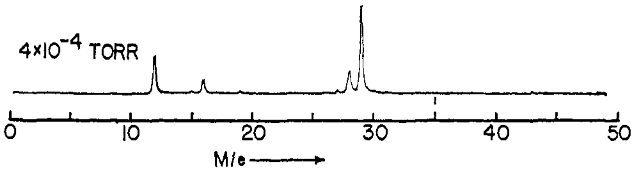

Figure 5. Single-resonance spectrum of chloroethylene with 70-ev electron energy at 4 × 10^{-4} torr. Drift voltage modulation gives the absorption line shape. No peaks were recorded above *m*/*e* 50.

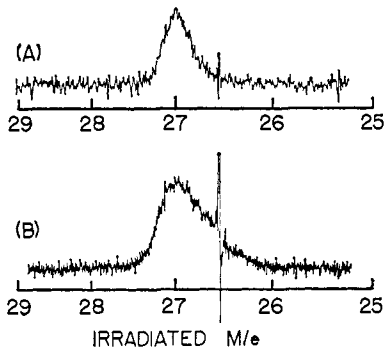

Figure 6. Pulsed double-resonance spectrum of the *m*/*e* 53 ($C_4H_5^+$) species with irradiation at the cyclotron frequency of $C_2H_3^+$. The irradiating power in spectrum B is increased 5 db over that used in spectrum A. The sharp feature at *m*/*e* 26$^1/_2$ is due to the irradiating oscillator exciting the first overtone of the marginal oscillator.

The chloroethylene (99.9% purity) and methane (ultrahigh purity grade, 99.95% purity) were obtained from Matheson and used without further purification. The perdeuteriomethane was obtained from Merck Sharp and Dohme of Canada.

III. Results

A. Variation of Single Resonance Spectra with Pressure. Figure 3 shows the appearance of the single-resonance icr spectra of chloroethylene obtained from 70-ev electrons at three different pressures with drift voltages set to approximately 1 v. The observing oscillator is operated at 153 kc/sec with ~0.01-v/cm radiofrequency level. Magnetic field modulation gives the derivative line shape. At 5 × 10^{-7} torr (Figure 3A) no reactions are observed, and the resulting spectrum corresponds closely to that obtained using a conventional mass spectrometer.[13] The only significant difference between the icr and conventional mass spectra at low pressure is the value of 4.8:1 obtained for the $^{35}Cl/^{37}Cl$ ratio in the parent ion in contrast with the expected value of 3:1.[13] No impurities other than a trace of argon at *m*/*e* 40 are evident.

At 5 × 10^{-6} torr (Figure 3B) numerous reaction products appear in the icr spectrum. The two chlorine isotopes serve as an aid in the identification of chlorine-containing reaction products. Analysis of the spectrum in Figure 3B indicates that the majority of the reac-

---

(13) "Mass Spectral Data," Manufacturing Chemists Association Research Project, Serial No. 122.

tion products are separated from parent ions by 26 mass units. This corresponds to the incorporation of a C_2H_2 group in the parent ion and suggests the general reaction

$$A^+ + C_2H_3Cl \longrightarrow AC_2H_2^+ + HCl \tag{6}$$

where A^+ is any of a number of ionic species present in the system. Figure 3C shows the chloroethylene mass spectrum at 3×10^{-5} torr. At this pressure the product ion intensity exceeds that of the parent ions.

All the observed *m/e* values and most likely ionic species to which they correspond are given in Tables I and II. The relative intensities of the major species at higher pressure are evident in Figure 3B and C.

Table I. Summary of Observed Ionic Species Appearing at Low Pressure

m/e	Species[a]	Relative intensity: Icr spectrum[b] (5×10^{-7} torr)	Relative intensity: Conventional mass spectrometer[c]
24	C_2^+	2.6	3.95
25	C_2H^+	10.4	13.78
26	$C_2H_2^+$	28.7	34.0
27	$C_2H_3^+$	100.0	100.0
35	$^{35}Cl^+$	6.8	8.76
36	$H^{35}Cl^+$	6.5	1.98
37	$^{37}Cl^+$	2.4	2.83
38	$H^{37}Cl^+$	2.1	0.65
47	$C^{35}Cl^+$	5.0	4.23
48	$CH^{35}Cl^+$	2.7	1.77
49	$C^{37}Cl^+$	1.6	1.48
50	$CH^{37}Cl^+$	0.9	0.63
59	$C_2{}^{35}Cl^+$	0.9	1.42
60	$C_2H^{35}Cl^+$	4.1	4.62
61	$C_2H_2{}^{35}Cl^+$, $C_2{}^{37}Cl^+$	7.4	6.87
62	$C_2H_3{}^{35}Cl^+$, $C_2H^{37}Cl^+$	84.8	76.6
63	$C_2H_2{}^{37}Cl^+$	3.0	3.80
64	$C_2H_3{}^{37}Cl^+$	17.7	24.2

[a] Contributions attributed to ^{13}C isotope neglected. [b] Data taken from spectrum shown in Figure 3A. [c] "Mass Spectral Data," Manufacturing Chemists Association Research Project, Serial No. 122. Instrument: Consolidated No. 21-103 mass spectrometer.

Table II. Summary of Observed Ionic Species Appearing at High Pressure

m/e	Species	*m/e*	Species
2	H_2^+	89	$C_4H_6{}^{35}Cl^+$
3	H_3^+	90	$C_4H_5{}^{37}Cl^+$
12	C^+	91	$C_4H_6{}^{37}Cl^+$, $C_7H_7^+$
16	CH_4^+	101	$C_5H_6{}^{35}Cl^+$
28	$C_2H_4^+$, CO^+	103	$C_5H_6{}^{37}Cl^+$
29	$C_2H_5^+$, COH^+	105	$C_8H_9^+$
39	$C_3H_3^+$	109	$C_3H_3{}^{35}Cl^{35}Cl^+$
53	$C_4H_5^+$	111	$C_3H_3{}^{35}Cl^{37}Cl^+$
63	$C_2H_4{}^{35}Cl^+$	113	$C_3H_3{}^{37}Cl^{37}Cl^+$
65	$C_2H_4{}^{37}Cl^+$, $C_5H_5^+$	114	$C_6H_7{}^{35}Cl^+$
73	$C_3H_2{}^{35}Cl^+$	115	$C_6H_8{}^{35}Cl^+$
75	$C_3H_4{}^{35}Cl^+$	116	$C_6H_7{}^{37}Cl^+$
77	$C_3H_4{}^{37}Cl^+$	117	$C_6H_8{}^{37}Cl^+$
79	$C_6H_7^+$	125	(?)
83	$CH^{35}Cl^{35}Cl^+$	127	$C_7H_8{}^{35}Cl^+$
85	$CH^{35}Cl^{37}Cl^+$	129	$C_7H_8{}^{37}Cl^+$
87	$CH^{37}Cl^{37}Cl^+$		
88	$C_4H_5{}^{35}Cl^+$		

At 11-ev electron energy no fragmentation occurs and only the parent ion is observed. As the pressure is raised it becomes possible to observe reactions of the parent ion exclusively. Figure 4 shows the appearance of the single-resonance spectrum obtained with 11-ev electrons at 3×10^{-6} torr. No mass peaks of significant intensity were observed below *m/e* 50. The drift voltages are again set to approximately 1 v in the source and resonance regions of the cell. The absence of the $C_2H_4Cl^+$ peak at 11 ev suggests that its mode of formation involves $C_2H_3^+$ in the reaction

$$C_2H_3^+ + C_2H_3Cl \longrightarrow C_2H_4Cl^+ + C_2H_2 \tag{7}$$

The other peaks in Figure 4 relate closely to those observed at 70 ev. The $^{35}Cl:{}^{37}Cl$ ratio observed in the parent ion with 11-ev electrons is 4.2:1. At 4×10^{-4} torr the only major peaks in the low mass region occur at *m/e* 12, 16, and 29 as shown in Figure 5. The resonances could correspond to C^+, CH_4^+, and $C_2H_5^+$ or HCO^+. No other peaks were observed up to *m/e* 130. Above 4×10^{-4} torr the spectra become appreciably collision broadened[14] and the mass resolution is poor.

B. Identification of Reactions. The two reactions 6 and 7 were inferred by the usual techniques[2] of varying pressure and electron energy. It is evident in Figure 4 that a fairly complex sequence of reactions occurs starting simply with the addition of the parent ion to the parent neutral. The application of double-resonance techniques directly demonstrates whether or not suspected reactions occur. In the pulsed double-resonance scheme the intensity of the product peak is monitored while the pulsed irradiating field is swept. Figure 6 demonstrates the pulsed double-resonance spectrum of the *m/e* 53 peak. A change is noted when the *m/e* 27 peak is irradiated. As the irradiating power is increased from Figure 6A to Figure 6B by a factor of 5 db, the width of the pulsed double-resonance spectrum increases from 0.3 to 0.6 mass unit, corresponding to an increased heating of the reactant ion. The sharp feature at *m/e* $26^1/_2$ corresponds to the spurious excitation of the first overtone of the marginal oscillator–detector by the irradiating oscillator.

The reaction thus identified is the first of the sequence

$$C_2H_3^+ + C_2H_3Cl \longrightarrow C_4H_5^+ + HCl \tag{8a}$$

$$C_4H_5^+ + C_2H_3Cl \longrightarrow C_6H_7^+ + HCl \tag{8b}$$

$$C_6H_7^+ + C_2H_3Cl \longrightarrow C_8H_9^+ + HCl \tag{8c}$$

in which all reactions are of the general type (6) and have been confirmed by double resonance. This sequence is of course also eliminated if 11-ev electrons are used. Reaction 8b is, however, only one of the reactions yielding the species $C_6H_7^+$. At higher pressures the $C_8H_9^+$ species exhibits only a small fraction of the intensity attained at intermediate pressures by $C_4H_5^+$ or $C_6H_7^+$. Double resonance also confirms reaction 7 which is followed by the sequence

$$C_2H_4Cl^+ + C_2H_3Cl \longrightarrow C_4H_6Cl^+ + HCl \tag{9a}$$

$$C_4H_6Cl^+ + C_2H_3Cl \longrightarrow C_6H_8Cl^+ + HCl \tag{9b}$$

where again the reactions are of type 6. The mass pattern between *m/e* 62 and 65 is repeated 26 mass units higher. This is shown clearly in Figure 7A. Figure 7B shows the pulsed double-resonance spectrum resulting from sweeping the magnetic field with $\omega_1/\omega_2 = 62/88$. Thus when the ion of *m/e* 88 is being observed, the ion of *m/e* 62 is being irradiated. This permits ob-

---

(14) J. L. Beauchamp, *J. Chem. Phys.*, **46**, 1231 (1967).

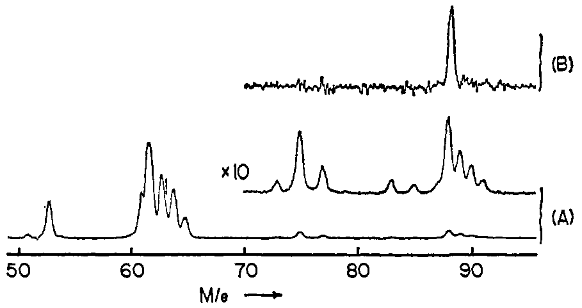

Figure 7. (A) Field-sweep single-resonance spectrum of chloroethylene with 70-ev electron energy at 5 × 10^{-6} torr. Drift voltage modulation gives the absorption line shape. (B) Field-sweep pulsed double-resonance spectrum. ω_1/ω_2 is fixed in the ratio 62/88.

servation of the reaction

$$C_2H_3{}^{35}Cl^+ + C_2H_3Cl \longrightarrow C_4H_5{}^{35}Cl^+ + HCl \quad (10)$$

and gives the single peak in Figure 7**B**. The resolution with drift modulation is not as good as that obtained with field modulation.

The reactions of the parent ion are best examined with 11-ev electron energy where no fragments other than the parent ion are formed. It is of interest to extend the identification of reaction 10 to examine the origin of the chlorine retained in the product ion. The resonances of the ^{35}Cl- and ^{37}Cl-containing species of both the reactant and product ions are well resolved. Thus it is possible to observe the ^{37}Cl-containing product with irradiation of the ^{35}Cl and ^{37}Cl reactants, or to observe the ^{35}Cl-containing product with irradiation of the ^{35}Cl- and ^{37}Cl-containing reactants. The relative intensities of these double-resonance spectra will depend in a simple way (as discussed in section IV) on the probability that the Cl atom from either the ionized or neutral reactant is retained in the product ion. Figure 8C displays the pulsed double-resonance spectrum of $C_4H_5{}^{37}Cl^+$. It is apparent that both $C_2H_3{}^{35}Cl^+$ and $C_2H_3{}^{37}Cl^+$ contribute to the product containing the ^{37}Cl isotope. Figure 8D displays the relative contribution of the parent ions to $C_4H_5{}^{35}Cl^+$. Similar behavior is observed in the reaction

$$C_2H_3Cl^+ + C_2H_3Cl \longrightarrow C_3H_4Cl^+ + CH_2Cl \quad (11)$$

where the results of observing $C_3H_4{}^{37}Cl^+$ and $C_3H_4{}^{35}Cl^+$ while irradiating the parent ions are shown in Figures 8A and **B**, respectively. For both reactions 10 and 11 the Cl atom in the product comes with equal probability from the charged or neutral reactant (section IV).

The peaks corresponding to $C_4H_6{}^{35}Cl^+$ (*m/e* 89) and $C_4H_6{}^{37}Cl^+$ (*m/e* 91) come primarily from $C_2H_4Cl^+$ at 70 ev *via* reaction 9a. At 11 ev no $C_2H_4Cl^+$ is formed, and the intensity of $C_4H_6Cl^+$ is diminished as shown in Figure 4 but does not entirely disappear. Figures 9A and **B** show respectively the pulsed double-resonance spectra for the *m/e* 89 and 91 ions at 11 ev and 70 ev under conditions such that only the principal secondary reactions are observed (Figure 3**B**). At 11 ev only the reaction

$$C_2H_3Cl^+ + C_2H_3Cl \longrightarrow C_4H_6Cl^+ + Cl \quad (12)$$

is observed. At 70 ev the double-resonance contributions from reaction 9a are also evident. At 11 ev and under conditions such that high order reactions are observed (Figure 4) the pulsed double-resonance spectrum of the *m/e* 91 ion (Figure 9C) is not nearly so straightforward; *m/e* 91 corresponds to $C_4H_6{}^{37}Cl^+$ and $C_7H_7{}^+$. The relative intensities of the *m/e* 89 and 91 peaks suggest that of the two ions with *m/e* 91, $C_7H_7{}^+$ makes a major contribution to the observed intensity. The pulsed double-resonance spectrum in Figure 9C shows a large contribution to *m/e* 91 from *m/e* 65. The *m/e* 65 ion, evident as a small peak in the single resonance spectrum of Figure 4, is quite reasonably $C_5H_5{}^+$ with the resulting reaction to give *m/e* 91 being

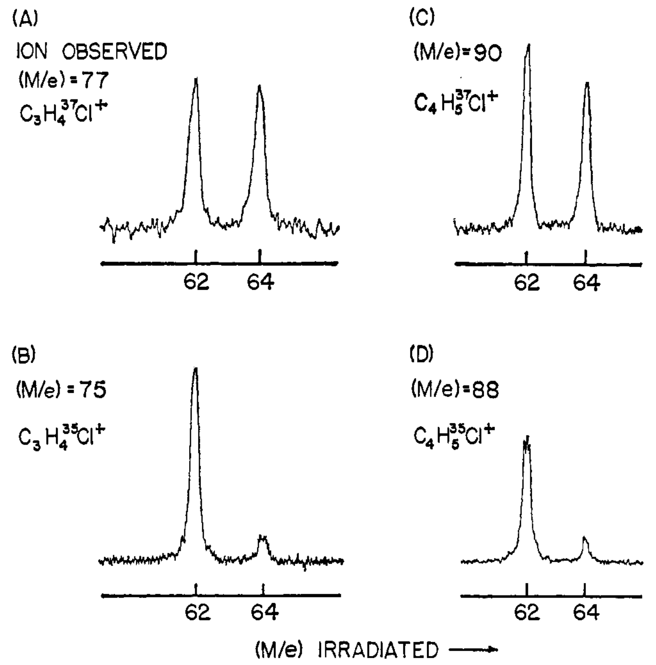

Figure 8. Pulsed double-resonance spectra showing the relative contributions of the parent chlorine isotopes to the product chlorine isotopes for $C_3H_4Cl^+$ and $C_4H_5Cl^+$ at 3 × 10^{-6} torr and 11-ev electron energy.

$$C_5H_5{}^+ + C_2H_3Cl \longrightarrow C_7H_7{}^+ + HCl \quad (13)$$

The *m/e* 65 to 75 relative intensity in the double-resonance spectrum shown in Figure 9C is much greater than the 65 to 75 intensity ratio in the single resonance spectrum of Figure 4. This suggests that although reaction 13 couples *m/e* 65 to *m/e* 91 in one step, the other observed contributions proceed to $C_7H_7{}^+$ through at least two or more successive reactions. $C_3H_4Cl^+$, for instance, must undergo a minimum of two reactions to form $C_7H_7{}^+$.

Figure 10 shows the relative contributions of the parent chlorine isotopes to the product ion isotopes in the reaction

$$C_3H_4Cl^+ + C_2H_3Cl \longrightarrow C_5H_6Cl^+ + HCl \quad (14)$$

The relative contributions of the parent chlorine isotopes to the product are similar to those observed in the two products examined in Figure 8. Table III summarizes the relative contributions of the parent isotopes to the product isotopes in the five reactions considered above which involve a single chlorine in both the parent and product ions.

Other reactions which have been observed and verified by double resonance include (at 70 ev)

$$CCl^+ + C_2H_3Cl \longrightarrow CHCl_2{}^+ + C_2H_2 \quad (15)$$

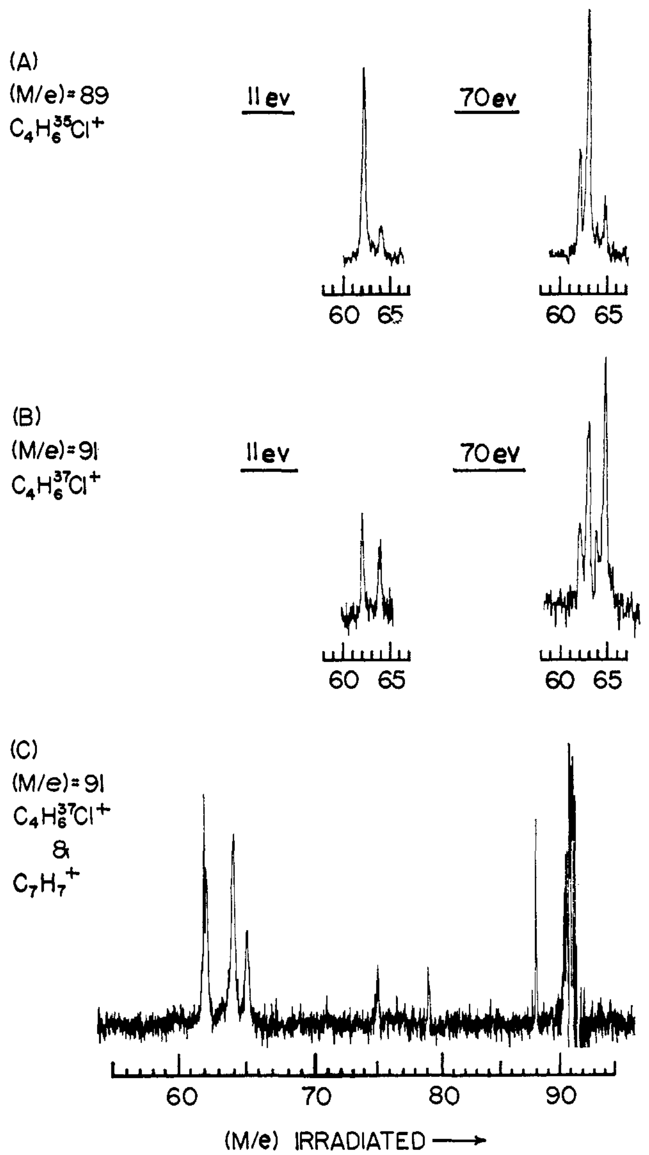

Figure 9. (A) and (B): Pulsed double-resonance spectra showing the relative contribution of the parent chlorine isotopes to the product chlorine isotopes for $C_4H_6Cl^+$ at 3 × 10^{-6} torr with 11 and 70 ev electron energy. (C): Pulsed double resonance spectra of *m/e* 91 products at 11 ev electron energy under conditions where high order reactions are observed.

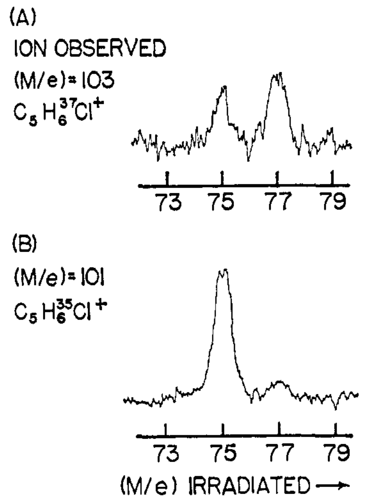

Figure 10. Pulsed double-resonance spectra showing the relative contributions of the $C_3H_4Cl^+$ ion chlorine isotopes to the chlorine isotopes in the $C_5H_6Cl^+$ product.

where $CHCl_2^+$ is evident in Figure 7A with isotopic peaks at *m/e* 83, 85, and 87 visible. The peak in Figure 7A at *m/e* 73 probably corresponds to $C_3H_2Cl^+$. Its double-resonance spectrum consists of contributions from the parent ion and *m/e* 89. The *m/e* 89 reaction can be written

$$C_4H_6{}^{35}Cl^+ + C_2H_3Cl \longrightarrow C_3H_2{}^{35}Cl^+ + C_3H_7Cl \qquad (16)$$

and the contribution from the parent ion may proceed through reaction 12 which produces $C_4H_6{}^{35}Cl^+$.

$C_6H_7^+$ is produced in the sequence 8a–c. However, it remains as a large peak at 11 ev, and double resonance shows it to come mostly from *m/e* 88 and 90, with small contributions from *m/e* 89 and 91. The postulated reaction involving $C_4H_5Cl^+$ is

$$C_4H_5Cl^+ + C_2H_3Cl \longrightarrow C_6H_7^+ + HCl + Cl \qquad (17)$$

while the reaction of $C_4H_6Cl^+$ involves the loss of two HCl functions.

$$C_4H_6Cl^+ + C_2H_3Cl \longrightarrow C_6H_7^+ + 2HCl \qquad (18)$$

It becomes increasingly difficult to sort out the reactions in the higher mass range. Products involving *m/e* values up to 127 are given in Table II. The ions corresponding to these peaks can in most cases be produced by addition of product ions above to chloroethylene followed by elimination of HCl.

Table III. Observed Relative Contribution of Reactant Ion Isotopic Species to Product Ion

Reactant	Product	Relative contribution of reactant ion isotopic species to product ion[a] ^{35}Cl	^{37}Cl
$C_2H_3Cl^+$	$C_3H_4{}^{35}Cl^+$	0.88	0.12
	$C_3H_4{}^{37}Cl^+$	0.57	0.43
$C_2H_3Cl^+$	$C_4H_5{}^{35}Cl^+$	0.85	0.15
	$C_4H_5{}^{37}Cl^+$	0.55	0.45
$C_2H_3Cl^+$	$C_4H_6{}^{35}Cl^+$	0.87	0.13
	$C_4H_6{}^{37}Cl^+$	0.57	0.43
$C_2H_4Cl^+$	$C_4H_6{}^{35}Cl^+$	0.85	0.15
	$C_4H_6{}^{37}Cl^+$	0.42	0.58
$C_3H_4Cl^+$	$C_5H_6{}^{35}Cl^+$	0.88	0.12
	$C_5H_6{}^{37}Cl^+$	0.46	0.54

[a] Sum of ^{35}Cl and ^{37}Cl relative contributions set equal to unity.

An attempt was made to observe exchange reactions of $^{35}Cl^-$ with $^{37}Cl^-$ and $^{35}Cl^+$ with $^{37}Cl^+$ *via* reactions of the type

$$^{35}Cl^{\pm} + C_2H_3{}^{37}Cl \longrightarrow C_2H_3{}^{35}Cl + {}^{37}Cl^{\pm} \qquad (19)$$

but neither of these reactions could be detected using double resonance. The charge exchange reaction

$$C_2H_3{}^{35}Cl^+ + C_2H_3{}^{37}Cl \longrightarrow C_2H_3{}^{37}Cl^+ + C_2H_3{}^{35}Cl \qquad (20)$$

however was detected using double-resonance techniques.

No cyclotron resonance absorption signals were observed which could be attributed to the intermediate species expected in the above reactions, and no effects were observed in the pulsed double-resonance spectra of the products with strong irradiation at the *m/e* values of the corresponding intermediates.

The prominent ion–molecule reaction sequences observed in the cyclotron resonance spectra of chloroethylene are summarized in Figure 11.

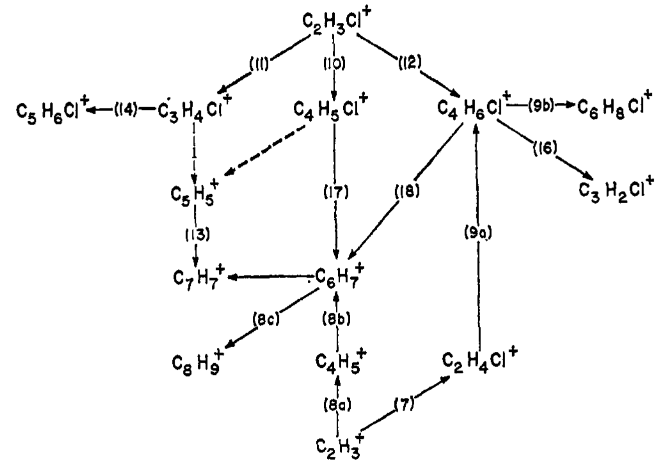

Figure 11 Reactions occurring in chloroethylene starting with $C_2H_3Cl^+$ and $C_2H_3^+$. The numbers refer to reactions in the text. The dashed lines indicate reactions which are inferred.

C. Mixtures of Chloroethylene with Methane and Methane-d_4. Figure 12 shows the spectrum of a mixture of methane and chloroethylene in the ratio 1:4. The products of two reactions known to occur in methane[15] are evident.

$$CH_4^+ + CH_4 \longrightarrow CH_5^+ + CH_3 \tag{21}$$

$$CH_3^+ + CH_4 \longrightarrow C_2H_5^+ + H_2 \tag{22}$$

Reactions discussed above characteristic of chloroethylene are also apparent. The behavior of the spectrum above *m/e* 60, where the peaks are distorted, is related to high ion densities in the resonance cell which result from low-drift velocities at high magnetic field strengths. Certain peaks in Figure 12 are the result of reactions between methane ions and chloroethylene neutrals. The reactions verified by double resonance include

$$CH_3^+ + C_2H_3Cl \longrightarrow C_3H_5^+ + HCl \tag{23}$$

$$C_3H_5^+ + C_2H_3Cl \longrightarrow C_5H_7^+ + HCl \tag{24}$$

$$C_2H_5^+ + C_2H_3Cl \longrightarrow C_4H_7^+ + HCl \tag{25}$$

Only one reaction between chloroethylene ions and methane neutrals was identified.

$$C_2H_3^+ + CH_4 \longrightarrow C_3H_5^+ + H_2 \tag{26}$$

This reaction is known to occur as a tertiary process in methane.[15]

Figure 13 gives the complex single resonance spectrum obtained with a mixture of chloroethylene and methane-d_4 in the ratio 4:1. Proton- and deuteron-transfer reactions combined with reactions of the type observed in methane and chloroethylene account for many of the peaks. The purpose of examining the mixture was to see if DCl or HCl would be eliminated in the reaction

$$CD_3^+ + C_2H_3Cl \longrightarrow \begin{array}{l} C_3H_2D_3^+\,(m/e\ 44) + HCl \\ C_3H_3D_2^+\,(m/e\ 43) + DCl \end{array} \tag{27}$$

Irradiating the CD_3^+ caused a change in the absorptions observed at both *m/e* 43 and 44. Since the peaks at *m/e* 43 and 44 had other contributions (none of which involved CD_3^+ as a precursor) the relative yields of HCl and DCl in reaction 27 could not be accurately estimated. These reactions confirm the generality of reaction 6. Since in the addition reaction of CD_3^+ both HCl and DCl are eliminated, it appears that proton transfers can occur very rapidly in the intermediate species. Rapid proton and deuteron transfers in intermediate species have been observed in the reaction of CD_4^+ with ethylene.[16]

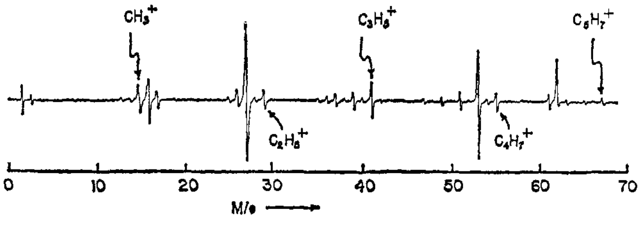

Figure 12. Field-sweep single resonance spectrum of a 4:1 mixture of chloroethylene and methane at 70-ev electron energy and 2×10^{-5} torr. Above *m/e* 62 peaks are distorted due to high ion densities.

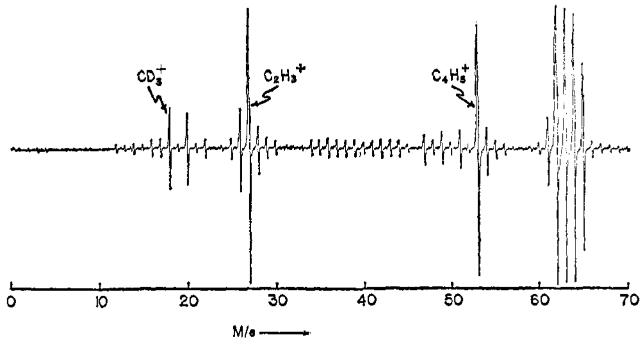

Figure 13. Field-sweep single-resonance spectrum of a 4:1 mixture of chloroethylene and perdeuteriomethane at 70-ev electron energy and 2×10^{-5} torr.

IV. Discussion

A. Single-Resonance Spectra. There are several obvious advantages to observing directly ion-molecule reactions in their reactant mixtures at pressures below 10^{-4} torr. First, the reactions are with certainty bimolecular. Secondly, there is no need to extract ions for analysis thereby precluding interferences which may occur during the extraction process. Thirdly, the static electric fields in the cell do not produce a net acceleration of the ions with the result that reactions are observed either at thermal energies or at translational temperatures determined by the initial fragmentation following electron impact. Finally, the direct observation of the ion-molecule mixture is an essential requirement for the application of the double-resonance scheme for the identification of reactions. The resolution at 10^{-4} torr is >100 and can be simply improved by operation at higher magnetic field. At 3×10^{-5} torr the spectrum in Figure 3C shows no overlapping of adjacent mass peaks as high as *m/e* 127.

The cyclotron resonance line shape in the absence of terms which couple the equation of motion of various ionic species is Lorentzian[14]

$$A(\omega) = \frac{\dfrac{ne^2E_0^2\nu}{4m}}{\nu^2 + (\omega - \omega_c)^2} \tag{28}$$

---

(15) F. P. Abramson and J. H. Futrell, *J. Chem. Phys.*, **45**, 1925 (1966).

(16) F. W. Lampe and F. H. Field, *Tetrahedron*, 7, 189 (1959).

where $A(\omega)$ is the power absorption, n is the number of ions, and ν is the collision frequency for momentum transfer. The absorption intensity varies inversely as the mass of the ionic species. If an icr spectrum is obtained by sweeping the magnetic field, the drift velocity of the ions in the cell changes according to eq 5 making n in eq 28 proportional to H and thereby to M. If ν is independent of the nature of the ionic species, then $A(\omega)$ should be an approximate measure of relative ion densities for a field-sweep spectrum. The general agreement of the low-pressure spectrum in Figure 3A with ref 13 substantiates these contentions. Difficulties are occasionally encountered when ion densities become sufficient for ion–ion interactions to distort the line shapes by disturbing the normal ion motions. The usual result is to give the line shape exhibited by the m/e 62 peak in Figure 12. The normal line shape can be obtained by lowering the electron emission current.

The variation of spectra with pressure as outlined in section IIIA is straightforward with the exception of the "high"-pressure spectrum at 4×10^{-4} torr shown in Figure 5 and the ^{35}Cl:^{37}Cl ratio in the parent ions. The species that remain at 4×10^{-4} torr appear to be remaining impurities and/or ions of unusual stability with regard to reaction with chloroethylene. At this pressure no parent or product ion evident at lower pressures could be observed.

With regard to the Cl isotope ratio it has been shown[14] in the case of a mixture of ^{20}Ne and ^{22}Ne isotopes that the single resonance spectrum will give an apparent value for the ratio of $^{20}Ne^+:^{22}Ne^+$ which exceeds the ratio of the corresponding neutral species by as much as a factor of 4. The mechanism for this is related to the way in which the charge-transfer cross sections vary with the ion–molecule relative velocity. If a similar mechanism were operating in the case of the $C_2H_3{}^{35}Cl^+$ and $C_2H_3{}^{37}Cl^+$ ions, then the observed ratio $C_2H_3{}^{35}Cl^+:C_2H_3{}^{37}Cl^+$ could be greater than 3:1. As noted in section III, charge transfer between the two isotopes of the parent ion was observed. This may, however, not be important at 5×10^{-7} torr (Figure 3A). This leaves the observed ratio of $C_2H_3{}^{35}Cl^+:C_2H_3{}^{37}Cl^+$ to be attributed to an instrumental effect, possibly a consequence of the modulation-detection scheme. With drift modulation (see Figure 7) the ratio appears to be less than 3:1, although the resolution is poor. With field modulation no significant change of the ratio occurred with variation of modulation amplitude or frequency.

B. Significance of Observed Reactions in Chloroethylene. Reaction 6 appears to have considerable generality as a bimolecular electrophilic addition–elimination process governing reactions of ions with chloroethylene. The species which undergo this reaction with chloroethylene include both ions and ion radicals. At pressures above a few torr it might be expected that the intermediate species in reaction 6 could be stabilized by collisional deactivation. This is the case in the ion–molecule reactions occurring in the radiolysis of C_2H_4[17] where ionic addition produces species which are stabilized before fragmentation occurs. Evidence[17] for this is given by the appearance of a sequence of mass peaks corresponding to $(C_2H_4)_n{}^+$, indicating successive addition without intermediate fragmentation.

The most significant result of this study is the identification of the origin of the chlorine atom retained in the product ion for the reactions in which the parent ion also contains a single chlorine atom. If the retained chlorine is that originally present in the parent neutral, then the isotopic distribution in these product ions will be the same as the isotopic distribution in the parent neutral, regardless of the identity of the chlorine isotope present in the reactant ion. Under these conditions if a particular chlorine isotope in the product is observed while the irradiating oscillator is swept, the irradiated ions will yield the product isotope in the ratio of 3:1. If the chlorine isotope in the ion product is retained from the parent ion then a particular chlorine isotope in the product exhibits a double-resonance peak only when irradiating the parent ion containing the same isotope. A third simple case obtains when the two chlorines in the intermediate species become equivalent and can be eliminated with equal probability. An analysis of the double-resonance effects to be expected in this case indicates that the ^{35}Cl and ^{37}Cl reactant ions will give contributions in the double-resonance spectrum of the ^{35}Cl and ^{37}Cl products in the ratios 7:1 and 3:5, respectively. Table IV shows the relative contributions of irradiated parent isotopes to each product ion isotope for the three cases considered.

Table IV. Calculated Relative Contribution of Reactant Ion Isotopic Species to Product Ion

Origin of Cl retained in product ion	Product Cl isotope	Relative contribution of reactant ion isotopic species to product ion[a]	
		^{35}Cl	^{37}Cl
Both chlorines retained with equal probability	^{35}Cl	0.875	0.125
	^{37}Cl	0.375	0.625
Chlorine retained from parent ion	^{35}Cl	1.0	0.0
	^{37}Cl	0.0	1.0
Chlorine retained from parent neutral	^{35}Cl	0.75	0.25
	^{37}Cl	0.75	0.25

[a] Sum of ^{35}Cl and ^{37}Cl relative contributions set equal to unity.

Reactions of the Parent Ion. As discussed in section III there are three competing reactions for the parent ion. These are

$$C_2H_3Cl^+ + C_2H_3Cl \longrightarrow \begin{cases} C_3H_4Cl^+ + CH_2Cl & \text{(29a)} \\ C_4H_5Cl^+ + HCl & \text{(29b)} \\ C_4H_6Cl^+ + Cl & \text{(29c)} \end{cases}$$

A comparison of the results given in Table III for reactions 29a–c with different possibilities considered in Table IV indicates that either of the two chlorine atoms present in the intermediate species can be eliminated with equal probability. Resonant charge exchange during the formation of a collision complex can provide a simple Cl atom equilibration mechanism for these three reactions. Two-step processes such as the charge-transfer reaction (20) followed by one of reactions 29a–c can also affect the observed relative contributions of reactant ion isotopic species to product ions. These effects can be recognized by their characteristic pressure and radiofrequency field dependence and probably

---

(17) P. Kebarle, R. M. Haynes, and S. Searles, ref 4, Chapter 13.

account for some of the discrepancies in the comparison of Tables III and IV.

Further mechanistic information on the reactions could obviously be obtained by using specifically deuterated chloroethylene. Although primary mass spectra of the various dichlorocyclobutanes are not yet available it would be of great interest to see what relationship they bear to the three primary reaction products obtained from the addition of $C_2H_3Cl^+$ to C_2H_3Cl. The results of the reaction of ethylene parent ions with ethylene have yielded results[2a] which strongly suggest that the intermediate decomposes to give products roughly analogous in abundance to those obtained in fragmentation of cyclobutane following electron impact. The reactions observed are

$$C_2H_4^+ + C_2H_4 \longrightarrow \begin{cases} C_3H_5^+ + CH_3 & (30a) \\ C_4H_6^+ + H_2 & (30b) \\ C_4H_7^+ + H & (30c) \end{cases}$$

which are analogous to reactions 29a–c. Similar results have been obtained in the case of tetrafluoroethylene.[18] The evidence in all three cases suggests that the intermediate species formed in the reaction of parent ethylenic ions with the corresponding neutral molecule are strongly bonded entities.

Higher Order Reactions. In reaction 14 the observation of chlorine isotope transfers indicates (Table III) equivalence of the chlorine in the intermediate species. In this reaction the possibility of charge exchange in the collision complex leading to equilibration is eliminated, and the effect must be attributed to the formation of an intermediate species $(C_5H_7Cl_2^+)^*$ in which the chlorines are positioned at chemically equivalent sites. In reaction 9a equivalence of the chlorines in the intermediate species is again indicated (Table III), suggesting the possibility of rapid resonant proton transfer between the ionic and neutral reactants during the formation of the collision complex. Chlorine isotope effects were not examined in the remaining higher order reactions because of the increasing complexity of competing reactions.

The formation of stable ionic species interrupts the general pattern of successive addition elimination reactions. The intensity of the $C_6H_7^+$ peak is quite large even at low pressures (Figures 3B and 4). This is probably the result of cyclization reactions producing protonated benzene (I). The fact that $C_7H_7^+$ is produced in a number of reactions is also indicative of its high stability, suggesting that the ion has the tropyllium structure (II).

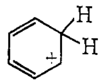
I

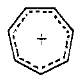
II

V. Conclusion

The above results quite clearly demonstrate the unique usefulness of ion cyclotron resonance for the study of ion–molecule reactions. The double-resonance technique used to follow the identity of chlorine isotopes is of course directly applicable to many reactions other than those studied here.[19] It is apparent that this technique can provide valuable information on the mechanisms of high-order ion–molecule reactions in complex systems and yield in addition qualitative evidence on the nature of reactive intermediates.

Acknowledgment. The authors wish to acknowledge the support of the National Science Foundation through Research Grant GP-4924. Additional support was provided by the Center for Materials Research at Stanford University. We wish to thank John V. Garcia for his technical assistance. The basic cyclotron resonance spectrometer used in this work was designed by Dr. Peter Llewellyn of Varian Associates, Palo Alto, California.

---

(18) G. A. W. Derwish, H. Galli, A. Giardini-Guidoni, and G. G. Volpi, *J. Am. Chem. Soc.*, **86**, 4563 (1964).

(19) J. L. Beauchamp and S. Sample, to be published.